

# Decapeptide Agonists of Human C5a: The Relationship between Conformation and Spasmogenic and Platelet Aggregatory Activities†

Sam D. Sanderson,\*‡ Leonid Kirnarsky,‡ Simon A. Sherman,‡ Julia A. Ember,§ Angela M. Finch,‡ and Stephen M. Taylor‡

*Eppley Institute for Research in Cancer and Allied Diseases, University of Nebraska Medical Center, 600 South 42nd Street, Omaha, Nebraska 68198-6805, Department of Immunology, Scripps Research Institute, 10666 North Torrey Pines Road, La Jolla, California 92037, and Department of Physiology and Pharmacology, University of Queensland, St. Lucia, QLD 4072, Australia*

Received April 22, 1994<sup>®</sup>

A series of decapeptide analogues corresponding to the C-terminal region of human C5a anaphylatoxin (C5a<sub>65-74</sub>) was synthesized with residue substitutions to restrict conformational flexibility in the C-terminus. These conformationally constrained peptides behaved as agonists of C5a in spasmogenic assays (smooth muscle contraction in human fetal artery, guinea pig ileum, and guinea pig lung parenchyma) as well as guinea pig platelet aggregation. There were significant correlations in the potencies of these peptides between the various assays. A structure–function analysis led to the identification of a preferred backbone conformation that correlated with the expression of these biological responses. These backbone structural motifs were consistent with a helix-like conformation for residues 65–69, an elongated structure for residues 70–71, and a  $\beta$ -turn of either type II or type V for residues (71)72–74. The most potent of these agonists expressed almost 5% of the potency of natural C5a.

## Introduction

The human anaphylatoxin C5a is a 74-residue glycopolypeptide that is generated by the enzymatic cleavage of the fifth component (C5) during plasma complement activation. C5a is recognized as a principal mediator of local and systemic inflammatory responses because of its ability to activate and recruit neutrophils,<sup>1</sup> induce spasmogenesis,<sup>2</sup> increase vascular permeability,<sup>3–5</sup> and stimulate the release of secondary inflammatory mediators from a variety of cell types.<sup>6–8</sup> C5a also appears to play a role in the modulation of immune response because of its ability to induce directly or indirectly the synthesis and release of the cytokines interleukin-1 (IL-1), interleukin-6 (IL-6), interleukin-8 (IL-8), and tumor necrosis factor- $\alpha$  (TNF- $\alpha$ ) from human monocytes.<sup>9–12</sup> These inflammatory and immunomodulatory activities are expressed via a transmembrane, G-protein-mediated signal transduction mechanism when the C5a ligand interacts with its receptor(s) expressed on the surface of certain circulating and tissue cell types.<sup>13–16</sup>

Because of its proinflammatory activity, C5a has been implicated as a pathogenic factor in the expression of certain inflammatory disorders such as rheumatoid arthritis,<sup>17</sup> adult respiratory distress syndrome,<sup>18,19</sup> gingivitis,<sup>20</sup> and the tissue damage associated with atherosclerosis and myocardial infarction.<sup>21,22</sup> Consequently, there is considerable interest in developing a specific C5a antagonist for use as an antiinflammatory agent in the treatment of these diseases.

One approach to the development of a C5a antagonist has focused on the synthetic manipulation of peptides possessing sequence homology to the C-terminal “effector” region of natural C5a. These peptides have been shown to be effective agonists compared to the parent polypeptide, but at markedly reduced potencies.<sup>12,23,24</sup> Therefore, a first step toward the development of an antagonist has been to increase the potency of these agonist peptides to a level approaching that of natural C5a, the rationale being that the increase in potency would reflect a heightened affinity for the C5a receptor. A potent, high affinity peptide could then serve as a template from which an analogue or mimetic might be developed that would retain the high affinity binding characteristics, so as to compete with natural C5a for the receptor, but not transduce a biological signal when bound to the receptor. This “ligand” approach has generated numerous agonist analogues that express a variety of biological activities and potencies, some of which have been used as probes of C5a pharmacology.<sup>25</sup> However, an effective peptide-based C5a antagonist has yet to be clearly described. In order to propose a rational design strategy for the generation of a high affinity/high potency template analogue, it is necessary to elucidate the relationship between the structural features expressed by a C-terminal agonist peptide and their biological consequences.

The general spatial arrangements of the N-terminal region of human C5a (residues 1–63) have been determined on the basis of <sup>1</sup>H-NMR data, but no definable spatial structure could be assigned to the C-terminal “effector” region (residues 64–74),<sup>26</sup> which appeared more flexible than the rest of the C5a polypeptide. However, based on a detailed analysis of the sequential *d*-connectivities from the original NMR data on human C5a,<sup>26</sup> we were able to distinguish three general structural features of the C-terminal decapeptide region, C5a<sub>65-74</sub> (ISHKDMQLGR). The region comprised of residues Ile-65 to Asp-69 was consistent with a twisted,

† This work is supported by grants from the Nebraska Cancer and Smoking Disease Research Program no. 94-40 to S.A.S. and no. 93-42 to S.D.S. and NCI CA3G727, ACS SIG-16, an American Heart Association Fellowship to J.A.E., and an NSRG grant to S.M.T. from the University of Queensland.

\* Author to whom correspondence should be addressed.

‡ University of Nebraska Medical Center.

§ Scripps Research Institute.

¶ University of Queensland.

® Abstract published in *Advance ACS Abstracts*, August 15, 1994.

helix-like structure, and the region made up of Met-70 to Gln-71 possessed an elongated backbone conformation. The C-terminal region of C5a<sub>65-74</sub>, comprised of residues Leu-72 to Arg-74, was considerably more flexible than the rest of the peptide and appeared to be made up of overlapping structural contributions of both twisted and elongated conformations. Flexibility in the C-terminal region (residues 71-74) appears to be important in the expression of biological activity because dramatic changes in activity and potency have been observed when the flexibility in this region was restricted.<sup>23,27,28</sup>

Thus, in order to develop rational design strategies that utilize these C-terminal agonist peptides, it is necessary to determine the conformational features within the C-terminal, flexible region of these decapeptides and to understand the role they play in the expression of biological activity. In this light, it is now possible to use the backbone conformational motifs described above for the decapeptide C5a<sub>65-74</sub> as a frame of reference to search for the biologically active conformation(s) and to rationalize the design for more potent and selective decapeptide agonist analogues of C5a.

In this paper, we report the results of a structure-function analysis of a panel of decapeptide analogues of human C5a<sub>65-75</sub> synthesized with residue substitutions that restrict flexibility in the C-terminal region of the peptide (residues 70-74). These conformationally constrained analogues were generated in order to determine the most likely conformation(s) that are responsible for the expression of spasmogenic activity in human fetal artery, guinea pig ileum, and guinea pig lung parenchyma and for aggregatory activity of guinea pig platelets. For the expression of these biological responses, we identified a characteristic C-terminal, turn-like motif that was consistent with a  $\beta$ -turn of type II or V for the region comprising residues 71-74. Moreover, analogues that expressed a structural propensity to this C-terminal motif appeared particularly potent relative to C5a in this class of biological assays. This study is a step toward the identification of distinct conformational features that appear to play a unique role in the expression of particular patterns of biological responses. The characterization of these conformational features will contribute to the generation of pharmacophore models that may assist in antagonist design strategies and help explain the observed variability in the biological activities expressed by C-terminal agonist peptides in different cellular and tissue systems.<sup>23,25,27,28</sup>

## Results and Discussion

**Conformational Characterization.** On the basis of the solution NMR data on human C5a, the tertiary structure for the region 1-63 was derived from the analysis of long- and medium-ranged nuclear Overhauser effects (NOE).<sup>26</sup> For the C-terminal region 64-74, however, long-range NOEs were not observed. Neither were there any observable NOEs between this C-terminal region and other parts of the polypeptide. Moreover, quantitative NOE interpretation was complicated by spectral overlaps. This region of C5a, therefore, was interpreted to be made up of flexible, random structure.

In order to determine the probable backbone conformations within the flexible region of human C5a re-

presented by the C-terminal ten residues (C5a<sub>65-74</sub>), we applied a probabilistic approach<sup>29</sup> that utilized the FISINOE program.<sup>30</sup> Input data to the FISINOE program came from the presence and/or absence of sequential *d*-connectivities from the original <sup>1</sup>H-NMR data on human C5a.<sup>26</sup>

The simultaneous presence of sequential *d*<sub>αN</sub>- and *d*<sub>NN</sub>-connectivities in the region (64)65-69 as well as *d*<sub>αβ</sub> (*i*, *i* + 3) was consistent with this region of C5a adopting a helix-like backbone conformation.<sup>29-31</sup> The region 70-71 was characterized by the presence of *d*<sub>αN</sub>-connectivities and the absence of *d*<sub>NN</sub>-connectivities, suggestive of an elongated backbone conformation.<sup>29-31</sup> The C-terminal end (residues 72-74) was characterized by the presence of *d*<sub>αN</sub>- and *d*<sub>NN</sub>-connectivities and by the absence of medium- and long-range NOEs, a pattern consistent with the dynamic averaging of an ensemble of structures with overlapping contributions made by elongated and twisted backbone conformations.<sup>29-31</sup> Thus, the NMR-matched, backbone conformational features of the C-terminal 10-residue region of C5a (C5a<sub>65-74</sub>) can be described as consisting of twisted, helix-like conformation for residues 65-69, elongated conformation for residues 70-71, and flexible structure of overlapping contributions made by twisted and elongated conformations in the C-terminal region 72-74.

It is assumed that the one (or more) biologically active conformation(s) of the C-terminal decapeptide C5a<sub>65-74</sub> lies within a low energy ensemble of conformers generated by the sterically allowable range of flexibility within the C-terminal end (residues 72-74). In fact, flexibility in this end of the peptide appears to be important for the expression of biological activity because activity is dramatically affected when this flexibility is restricted.<sup>23,27,28</sup> Thus, it is important to identify the conformational features in the C-terminal end of C5a<sub>65-74</sub> that relate to the expression of various biological activities.

We suggest the likelihood of a reverse or  $\beta$ -turn in the C-terminal region of (Gln-71 to Arg-74) of C5a<sub>65-74</sub> on the basis of three lines of evidence. First was the presence of overlapping twisted and elongated structure in this region as determined from our analysis of the NMR data of human C5a. Second was an increase in neutrophil membrane binding and chemotactic activity for certain C-terminal octapeptide analogues of C5a in which Gly-73 was substituted with D-Ala.<sup>32</sup> This, along with the position of the Gly in the four-residue reverse-turn stretch (*i* + 2, or -Gln-Leu-Gly-Arg), was suggestive of a  $\beta$ -turn that was stabilized by the D-Ala substitution. Indeed, the pattern of changes observed in the biological activity expressed by the conformationally constrained analogues described in this paper (see below) not only confirm the presence of a C-terminal, reverse-turn but correlate with a  $\beta$ -turn of type II or V for the biological responses tested (i.e., spasmogenic and platelet aggregatory activities).

**Peptide Characterization.** Table 1 summarizes the amino acid compositional and mass spectral analyses of the 23 peptide analogues used in this study. This panel is also listed in Table 2, which summarizes the biological results in human fetal artery and guinea pig platelets. Selected peptides are shown in Table 3, which summarizes the results in guinea pig ileum and lung

Table 1. Amino Acid Compositional and Mass Spectral Analysis of C5a Analogue Peptides<sup>a</sup>

Peptide No.	Amino Acids											Mass Spectral Results	
	Tyr	Ser	Phe	Lys	Asp	Met	Glx	Leu	Gly	Arg	Other	Theor.	Obs.
1.		0.85	1.01	0.99	1.04	0.77	1.12	1.16	1.06	1.12	1.00 (Ile)	1195	1195
		(1)	(1)	(1)	(1)	(1)	(1)	(1)	(1)	(1)	(1)		
2.	1.11	1.11	1.11	1.11	1.11	1.11	1.11	1.11	1.11	1.11		1245	1245
	(1)	(1)	(1)	(1)	(1)	(1)	(1)	(1)	(1)	(1)			
3.	1.05	0.86	1.04	0.93	1.07	0.96	1.07	1.04		1.02	0.95 (Pro)	1285	1285
	(1)	(1)	(1)	(1)	(1)	(1)	(1)	(1)		(1)	(1)		
4.	0.94	0.77	0.97	0.84	1.01	1.04	1.02		0.99	0.98	1.02 (Pro)	1228	1228
	(1)	(1)	(1)	(1)	(1)	(1)	(1)		(1)	(1)	(1)		
5.	1.00	0.99	0.98	1.08	1.05	0.86		0.99	1.00	0.99	1.07 (Pro)	1214	1214
	(1)	(1)	(1)	(1)	(1)	(1)		(1)	(1)	(1)	(1)		
6.	ND	ND	ND	ND	ND	ND			ND	ND	ND (Pro)	1198	1198
	(1)	(1)	(1)	(1)	(1)	(1)			(1)	(1)	(2)		
7.	1.06	0.83	1.05	0.99	1.07	0.90	0.96	1.08		1.03	0.99 (Ala)	1259	1259
	(1)	(1)	(1)	(1)	(1)	(1)	(1)	(1)		(1)	(1)		
8.	1.02	0.96	1.03	1.00	1.26	1.00	1.05	1.00		0.99	0.97 (D-Ala)	1259	1259
	(1)	(1)	(1)	(1)	(1)	(1)	(1)	(1)		(1)	(1)		
9.	1.03	0.97	0.98	0.89	1.09	1.02	1.04	0.96	1.06	0.97		1245	1245
	(1)	(1)	(1)	(1)	(1)	(1)	(1)	(1)	(1)	(1)			
10.	1.05	0.85	1.09	1.00	0.98	0.98		0.93		1.06	1.06 (D-Ala), 1.01 (Pro)	1228	1228
	(1)	(1)	(1)	(1)	(1)	(1)		(1)		(1)	(1)		
11.	1.06	0.78	1.09	0.88	0.98	1.05			0.92	1.11	1.10 (Ala), 1.12 (Pro)	1172	1172
	(1)	(1)	(1)	(1)	(1)	(1)			(1)	(1)	(1)		
12.	1.06	0.84	1.07	1.07	0.96	0.94				1.02	1.98 (D/L-Ala), 1.03 (Pro)	1186	1186
	(1)	(1)	(1)	(1)	(1)	(1)				(1)	(2)		
13.	0.92	0.71	2.06	0.99	1.00	1.01		0.98		1.28	1.04 (Pro)	1304	ND
	(1)	(1)	(2)	(1)	(1)	(1)		(1)		(1)	(1)		
14.	0.98	0.94	1.06	0.95	1.06	0.99		0.96		0.99	2.10 (D/L-Pro)	1254	ND
	(1)	(1)	(1)	(1)	(1)	(1)		(1)		(1)	(2)		
15.	1.10	0.89	1.07	0.97	0.96			0.94	1.00	1.01	1.04 (Ala), 1.04 (Pro)	1154	1154
	(1)	(1)	(1)	(1)	(1)			(1)	(1)	(1)	(1)		
16.	1.04	0.82	1.07	0.89	0.90			1.04	1.12	1.08	1.01 (Cys), 1.01 (Pro)	1186	1186
	(1)	(1)	(1)	(1)	(1)			(1)	(1)	(1)	(1)		
17.	1.06	0.98	1.08	0.98	0.93			0.91		1.05	2.10 (Cys), 1.10 (Pro)	1232	1232
	(1)	(1)	(1)	(1)	(1)			(1)		(1)	(2)		
18.	1.02	0.82	1.08	1.01	0.94			1.05		1.09	1.88 (Cys), 1.11 (Pro)	1230	1230
	(1)	(1)	(1)	(1)	(1)			(1)		(1)	(2)		
19.	0.97	0.80	1.06	0.95	1.04			1.01		1.04	2.05 (D/L-Ala), 1.04 (Pro)	1168	ND
	(1)	(1)	(1)	(1)	(1)			(1)		(1)	(2)		
20.	0.95	1.05	0.96	1.09		0.95		1.88	1.24	1.10		1172	ND
	(1)	(1)	(1)	(1)		(1)		(2)	(2)	(1)			
21.	0.99	0.99	1.10	1.22				2.75	1.92	1.09		1154	ND
	(1)	(1)	(1)	(1)				(3)	(2)	(1)			
22.	1.02	0.99	1.06	1.10		0.99		1.94	1.90	0.99		1172	ND
	(1)	(1)	(1)	(1)		(1)		(2)	(2)	(1)			
23.	1.00	0.83	1.09	1.02		0.98		0.93	2.19	0.94	1.00 (Pro)	1156	ND
	(1)	(1)	(1)	(1)		(1)		(1)	(2)	(1)	(1)		

<sup>a</sup> Values in parentheses are the expected number of residues, numbers directly above them are the observed. ND, not done.

parenchyma. All peptides were based on the C-terminal 10-residues of human C5a (C5a<sub>65-74</sub> or ISHKDMLGR) and on a more potent analogue (C5a<sub>65-74</sub>Y65,F67 or YSFKDMQLGR). The replacement of His at position 67 with the aromatic residue Phe (peptide 1, Table 2) was shown to afford about a 2 order of magnitude increase in potency relative to C5a<sub>65-74</sub>.<sup>33,34</sup> Tyr was used in place of Ile-65 in order to provide a site for radioactive iodination for tracer studies.<sup>41</sup> In smooth muscle contraction of human fetal artery, C5a<sub>65-74</sub>Y65,F67 was shown to be about 20 times more potent than the C-terminal 19-mer of natural sequence (C5a<sub>56-74</sub>) (Figure 1). Substituted residues that differ from those in C5a<sub>65-74</sub>Y65,F67 are shown in bold face (Table 2). All peptides were homogeneous by both analytical RP-HPLC and mass spectral analysis and gave the expected residue molar ratios by compositional analysis and parent ion molecular mass by FAB-MS (see Table 1).

Residue substitutions in C5a<sub>65-74</sub>Y65,F67 were chosen to restrict the flexibility in the C-terminal region of the decapeptide in order to bias certain features of backbone conformation that would be useful in the search for the biologically relevant conformation(s) in

the flexible, C-terminal region. Three principal types of modifications were employed. These include (1) Pro substitutions for restricting local  $\phi$  angle flexibility and for influencing the allowed conformations of the pre-proline residue, (2) Ala substitutions for evaluating the contributions made by the side chains in the peptide, and (3) D-residue substitutions for altering local stereoisometric arrangements. The changes in biological activity induced by these restrictions in C-terminal flexibility and conformational space alterations were assessed in spasmogenic assays (smooth muscle contraction in human fetal artery, guinea pig ileum, guinea pig lung parenchyma) and in guinea pig platelet aggregation.

**Pharmacological Activity.** Table 2 summarizes the pharmacological activities of human C5a, C5a<sub>65-74</sub>Y65,F67, and its analogues in the smooth muscle contraction of human fetal artery and the aggregation of guinea pig platelets. Table 3 summarizes the smooth muscle contractile responses of C5a and selected analogues in guinea pig ileum and guinea pig lung parenchyma. All analogues screened in these spasmogenic assays induced responses in a dose-dependent manner (see Figure 1, for example) and were shown to be full

**Table 2.** Pharmacological Activities of C5a Analogues in Human Fetal Artery and Guinea Pig Platelet Aggregation Assays

no.	peptide	fetal artery pD <sub>2</sub> + SE (n) <sup>a</sup>	EC <sub>50</sub> (μM) <sup>b</sup>	platelet aggreg (μM) <sup>c</sup>
	C5a	7.92 ± 0.09 (23)	0.018	0.023
1	ISFKDMQLGR	—	—	86.3
2	YSFKDMQLGR	5.05 ± 0.06 (26)	11.2	22.9
3	YSFKDMQLPR	<3 (3)	>1000	225
4	YSFKDMQPGR	4.40 ± 0.16 (4)	48.0	500
5	YSFKDMPLGR	6.18 ± 0.11 (20)	1.13	6.3
6	YSFKDMPPGR	4.68 ± 0.17 (4)	25.1	80
7	YSFKDMQLAR	4.04 ± 0.12 (11)	122	34
8	YSFKDMQLAR	5.42 ± 0.36 (7)	12.2	20
9	YSFKDMQIGR	3.77 ± 0.39 (3)	286	150
10	YSFKDMPLAR	6.57 ± 0.08 (16)	0.35	1.3
11	YSFKDMPAGR	<3 (3)	>1000	101
12	YSFKDMPAaR	4.86 ± 0.14 (6)	17.9	90
13	YSFKDMPLfR	4.53 ± 0.34 (4)	51.1	2.3
14	YSFKDMPLpR	5.57 ± 0.22 (4)	3.70	2.7
15	YSFKDAPLGR	6.11 ± 0.15 (12)	1.74	7.4
16	YSFKDCPLGR	5.79 ± 0.16 (6)	2.04	2.3
17	YSFKDCPLCR	4.67 ± 0.14 (8)	26.6	4.1
18	YSFKDCPLCR	<4 (3)	162	>410
19	YSFKDAPLaR	6.57 ± 0.15 (4)	0.33	0.54
20	YSFKGMLLGR	5.34 ± 0.10 (4)	4.9	10.5
21	YSFKGILLGR	5.21 ± 0.19 (2)	6.6	21
22	YSFKGMLLGR	4.43 ± 0.11 (4)	40.0	—
23	YSFKGMPLGR	6.23 ± 0.11 (4)	0.59	6.3

<sup>a</sup> Mean pD<sub>2</sub> ± SE values shown. (n) number of experiments.

<sup>b</sup> Mean EC<sub>50</sub> values derived from individual experiments. <sup>c</sup> The dilution of a peptide producing visible platelet aggregation (i.e., threshold response). Residue substitutions to peptide 2 shown in boldface.

agonists compared to natural C5a in these activities. Those peptides of very low potency (EC<sub>50</sub> > 1 mM), for which EC<sub>50</sub> values could not be accurately obtained, were tested for antagonist activity against C5a at concentrations below those that caused contraction or aggregation, but were without effect.

The spasmogenic effects of C5a are due to the release of secondary mediators such as histamine and eicosanoids from inflammatory cells. In guinea pig ileum, the major contractile mediator is histamine released from degranulating mast cells.<sup>35,36</sup> In human fetal artery and guinea pig lung parenchyma, cyclo-oxygenase metabolites mediate the contractile response, which is blocked by cyclo-oxygenase inhibitors.<sup>37,38</sup> Cyclo-oxygenase inhibitors also block the contractile response of the decapeptide analogues of C5a<sub>65-74</sub>Y65,F67 in these tissues (Finch, A.; Taylor, S. M., unpublished results), although the cell types involved in these latter tissues have not been identified. Mast cells are not present in human fetal artery, but there is some evidence that macrophages may be the cellular source of the eicosanoids released in this tissue.<sup>37</sup>

As shown in Table 2, restricting backbone flexibility at position 73 by substituting Pro at this position (peptide 3) was detrimental to spasmogenic and aggregatory activities compared to C5a<sub>65-74</sub>Y65,F67 (peptide 2). The same restriction at the adjacent position, Leu-72 (peptide 4) was also depressive to spasmogenic activity and platelet aggregation (Tables 2 and 3). These observations suggest that the topographical contribution made by the side chain of Leu-72 and/or the presence of some freedom of backbone flexibility at or near this position is important for the expression of biological activity.

Interestingly, a Pro substitution for Gln at position 71 (peptide 5) afforded a significant (4–10-fold) increase in potency in spasmogenic and aggregatory activities relative to peptide 2 (Tables 2 and 3). This suggests that the side chain of Gln is probably less influential in contributing to a biologically favorable topography and that more favorable topochemical/conformational features appear to result from restrictions in backbone flexibility at this position. This notion was supported by double-Pro substitutions in peptide 6. In this case, the decrease in potency observed by the presence of Pro at position 72, which was shown to adversely affect activity (see peptide 4), appeared to be offset by the presence of Pro at the more favorable position 71. The presence of the two Pro residues was not nearly as detrimental to biological activity as was the presence of the single Pro substitution for Leu at position 72 (peptide 4).

Modulating flexibility by increasing steric bulk via an Ala substitution for Gly at position 73 (peptide 7) had an adverse effect on spasmogenic and aggregatory activities compared to peptide 2. However, activity in both assays was completely restored to the level of peptide 2 when Ala-73 was replaced by D-Ala (peptide 8). Moreover, the presence of both D-Ala-73 and Pro-71 appeared to have an additive or complementary effect on activity. Indeed, peptide 10 was about 32-fold more potent than peptide 2 in spasmogenic activity and about 18-fold more potent in platelet aggregation. The peptide having both D-Ala-73 and Pro-71 (peptide 10) was substantially more potent than peptides that possessed either substitution alone (peptides 5 and 8). It also appeared that the size of the D-residue side chain at position 73 was important. The substitution of a bulky D-Phe at position 73 (peptide 13) had an adverse effect on spasmogenic activity, but appeared to benefit platelet aggregation. However, the substitution of a D-Pro at position 73 (peptide 14) had less of a detrimental effect on activity than did D-Phe at this position, but was not as beneficial as when D-Ala occupied position 73 (peptide 10). It is not clear whether this is the exclusive result of the presence of a D-residue at position 73 that lacks a bulky side chain or whether the presence of Pro at the more critical position 71 overrides any detrimental effects of having D-Pro at position 73 alone.

Unlike the favorable topochemical effect of D-Ala at position 73 (peptide 8), the replacement of Leu-72 with D-Leu (peptide 9) had an adverse effect on spasmogenic and aggregatory activities. These results were similar to that observed with peptide 4 in which Pro was substituted for Leu-72. Even in the presence of the highly favorable substitution of Pro-71, a relatively isosteric substitution of Ala for Leu-72 (peptide 11) was detrimental to activity. However, some recovery was observed when D-Ala occupies position 73 (peptide 12). These results point to the importance of the contribution made by the side chain of Leu-72 to the expression of a biologically favorable topography. Thus, the integrity of the side chain of Leu at position 72, a backbone restriction at position 71(Pro), and the presence of D-Ala at position 73 seems to confer particularly favorable, C-terminal topochemical features well suited to the potent expression of spasmogenic and platelet aggregatory activities.

Table 3. Pharmacological Activities of C5a Analogues in Guinea Pig Ileum and Lung Parenchyma

no.	peptide	ileum		lung parenchyma	
		$pD_2 \pm SE (n)^a$	$EC_{50} (\mu M)^b$	$pD_2 (n)^a$	$EC_{50} (\mu M)^b$
	C5a	$7.06 \pm 0.19 (8)$	0.16	$7.42 \pm 0.11 (5)$	0.043
2	<b>YSFKDMLGR</b>	$4.51 \pm 0.09 (9)$	37.5	$4.56 \pm 0.07 (4)$	28.4
4	<b>YSFKDMQPGR</b>	$3.64 \pm 0.24 (4)$	344		
5	<b>YSFKDMP LGR</b>	$5.14 \pm 0.19 (7)$	11.5	$5.15 \pm 0.14 (4)$	8.1
15	<b>YSFKDAP LGR</b>	$4.79 \pm 0.26 (4)$	26.6		
20	<b>YSFKGML LGR</b>	$4.61 \pm 0.18 (2)$	26.8	$5.00 \pm 0.24 (4)$	15.1
21	<b>YSFKG LLLGR</b>	$4.74 \pm 0.02 (2)$	18.1	$4.70 \pm 0.20 (2)$	22.1

<sup>a</sup> Mean  $pD_2 \pm SE$  values shown. ( $n$ ) number of experiments. <sup>b</sup> Arithmetic mean  $EC_{50}$  values derived from average of individual experiments. Residue substitutions to peptide 2 shown in boldface.

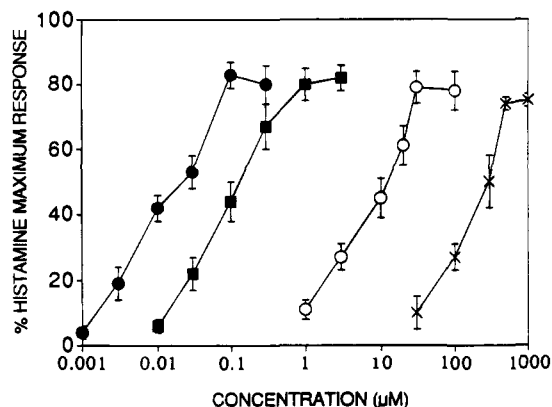


**Figure 1.** Dose-response curves for human recombinant C5a and agonist peptides in human fetal artery. Tissue strips were exposed to single concentrations of C5a or peptides and, following contraction, exposed to a supramaximal concentration of histamine ( $10 \mu M$ ). (●) C5a; (×) C-terminal 19-mer of natural sequence (VVASQLRANISHKDMQLGR); (○) peptide 2 (YSFKDMLGR), demonstrating the effect of substitution of Phe-67 for His-67; (■) peptide 10 (YSFKDMP LGR), showing the increased potency induced by the dual substitutions of Pro-71 and D-Ala-73. Points represent the mean response and the vertical bars the SEM.  $n = 6-8$  experiments in each group.

Recent NMR results on C5a<sub>65-74</sub>Y65,F67 (peptide 2) suggested that the alkyl side chain of Met-70 forms a hydrophobic cluster with the aromatic side chains of Tyr-65 and Phe-67 to stabilize a helical turn in the N-terminal region of the peptide (Carpenter, K.; Sanderson, S. D.; Ripoll, D.; Hugli, T. E.; Ni, F., unpublished results). However, shortening the alkyl side chain of Met-70 and diminishing its hydrophobic character by substituting either Ala (peptide 15) or Cys (peptide 16) had very little effect on activity compared to their homologue, peptide 5 (see also Table 3). The presence of Cys at position 73 in place of Gly (peptide 17), however, seemed to have a more substantial effect on decreasing spasmogenic potency, but not to the extent observed when the isostere Ala occupies this position (peptide 7). The formation of an extended disulfide bridge (peptide 18) that spans the flexible C-terminal region diminished biological potency well beyond that observed with the two reduced Cys present (peptide 17), implying that more global restrictions in flexibility might be less conducive to expressing a biologically favorable topography. These results suggest that the side chain of Met-70 probably plays a fairly minor role in contributing to the biologically favorable topography within the C-terminal region.

The biological correlations between spasmogenic and platelet aggregatory activities (Figures 4-6) suggest that a pharmacologically favorable backbone conforma-

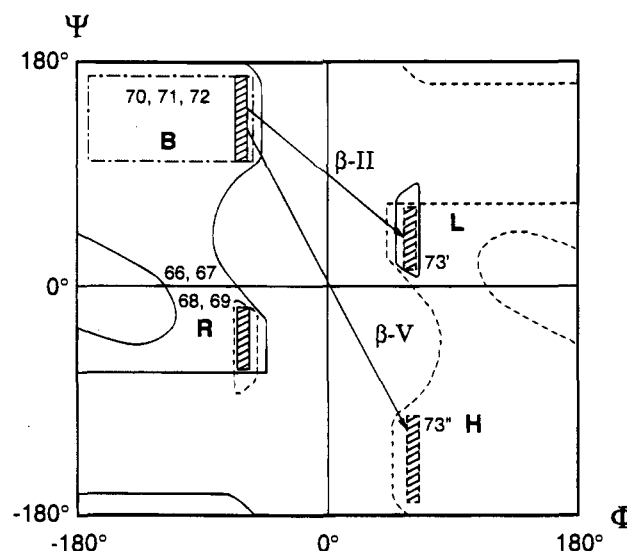


**Figure 2.** Ramachandran plot showing the sterically allowed conformational space occupied by the amino acid residues in the decapeptide C5a<sub>65-74</sub>. (The terminal residues 65 and 74 are omitted.) Sterically allowed space for L- and D-residues are contained within the solid and hashed lines, respectively. The narrow, vertical regions depict the allowed space for L-Pro (left hand quadrants outlined with solid lines) and D-Pro (right hand quadrants outlined with dashed lines). The boxed region in quadrant B is the allowable conformational space for the pre-proline residues. B, R, L, and H refer to the ( $\phi$ ,  $\psi$ ) regions that correspond to  $\beta$ -structure, right handed helices, left handed helices, and high energy structure, respectively.

tion/topography within the C-terminal region of C5a<sub>65-74</sub>Y65,F67 can be obtained by D-Ala substitution at position 73, maintaining the integrity of the side-chain of Leu at position 72, and Pro substitution at position 71 for backbone restrictions of flexibility at this site. Also, position 70 (Met) appears to provide a site that affords some leeway in the type of side chain one chooses to incorporate. This affords an interesting synthetic advantage, since it is now possible to substitute a nonoxidizable residue, Ala (peptide 15), at this position with no demonstrable effects on biological activity. The above biological results also imply that the simplest sequence within the flexible, signal transducing C-terminal region of C5a<sub>65-74</sub>Y65,F67 responsible for optimal expression of activity in these assays would be [YSFKD]APLaR. In fact, this analogue (peptide 19) was equipotent to peptide 10 in its spasmogenic activity and about twice as potent in platelet aggregation.

Peptides 20-23 are rat decapeptide homologues of peptides 2 and 5. The C-terminal octapeptide sequence of rat C5a is known,<sup>32</sup> and as shown in Table 2, the rat decapeptide homologue of peptide 2 (i.e., peptide 20) is

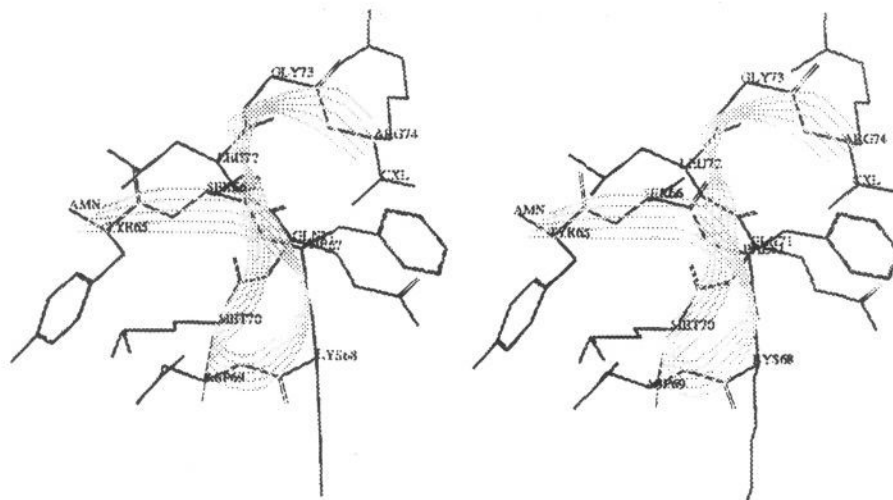


**Figure 3.** Stereoview of the decapeptide agonist C5a<sub>65-74</sub>Y<sub>65</sub>,F<sub>67</sub> (YSFKDMQLGR) showing the helix-like conformation for Tyr-65 to Asp-69, elongated conformation for Met-70 to Gln-71, and  $\beta$ -turn type II for (Gln-71)Leu-72 to Arg-74.

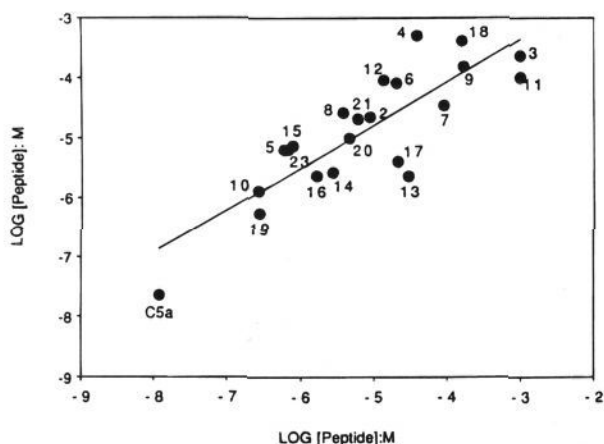


**Figure 4.** Correlation between effective peptide concentrations in fetal artery and platelet aggregation. Abscissa: mean  $pD_2$  values for peptides in fetal artery. Ordinate: Threshold concentration of peptides causing platelet aggregation. Regression coefficient ( $r$ ) = 0.84,  $n$  = 23.

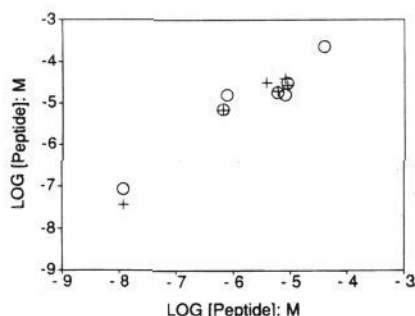


**Figure 5.** Correlation between  $pD_2$  values for peptides and C5a in fetal artery, ileum and lung parenchyma. Abscissa:  $pD_2$  values in fetal artery. Ordinate:  $pD_2$  values in ileum (○) and parenchyma (+). Data derived from Table 2. Fetal artery versus ileum,  $r$  = 0.95 ( $n$  = 7); fetal artery versus lung parenchyma,  $r$  = 0.98 ( $n$  = 5).

about 2 times more potent in human fetal artery and guinea pig platelet assays. The oxidizable Met at position 70 was substituted with Leu (peptide 21) with no significant changes in the spasmogenic assays and a slight decrease in platelet aggregation compared to peptide 20. Peptide 22 was substituted with a D-Arg

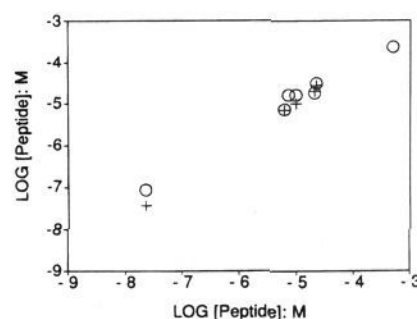


**Figure 6.** Correlation between effective concentrations for peptides and C5a in guinea pig platelets, ileum, and lung parenchyma. Abscissa: Threshold concentration causing platelet aggregation. Ordinate:  $pD_2$  values in ileum (○) and parenchyma (+). Data derived from Table 2. Platelet aggregation versus ileum,  $r$  = 0.99 ( $n$  = 7); platelet aggregation versus lung parenchyma,  $r$  = 0.99 ( $n$  = 5).

at position 74 to assess the possibilities of this analogue acting as an antagonist to natural C5a.<sup>25</sup> Peptide 22 remained a full agonist of diminished potency but was devoid of any antagonistic activity. Finally, peptide 23 is the rat homologue of peptide 5. As with peptide 5, the presence of Pro at position 71 seemed to bias a favorable backbone conformation, which was reflected in an increase in potency in fetal artery and platelet aggregation assays compared to peptide 20.

#### Analysis of Structure-Function Relationships.

As described above, our analysis of the sequential  $d$ -connectivities of the C-terminal 10 residues of natural C5a (C5a<sub>65-74</sub>) was consistent with a helix-like structure dominating residues 65/66-69 and an elongated backbone conformation for residues 70-71. On the basis of other lines of evidence, we proposed that the C-terminal residues 72-74 likely exist in a  $\beta$ -turn-like motif, but inherent flexibility in this region precluded the accurate assignment of a specific type of  $\beta$ -turn. In this study, we looked at the biological activities of a panel of peptides in which the flexibility of this C-terminal region has been restricted. The biological trends exhibited by these conformationally constrained analogues can now be used to obtain more precise information about the conformational features in the flexible, C-terminal region of these decapeptides (i.e., residues 71/72-74).

Analysis of the NMR data published for human C5a by the FINISOE program suggested that the decapeptide C5a<sub>65-74</sub> has helix-like conformation for the region comprised by residues 65/66-69, placing these residues in the region of allowed Ramachandran space at or near  $\phi = -90^\circ$  and  $\psi = 0^\circ$  within the B/R region (Figure 2). The elongated backbone conformation suggested for residues 70-71 would place them in the B quadrant ( $\phi = -90^\circ$  to  $-120^\circ$ ,  $\psi = 110^\circ$  to  $140^\circ$ ).

The incorporation of a Pro residue significantly narrows the range of sterically allowed backbone conformations of the preceding (preproline) residue.<sup>39</sup> Thus, a Pro substitution will fix the preproline residue in an elongated conformation by restricting  $\psi$  angle rotations within the narrow interval of about  $100^\circ$  to  $160^\circ$  (i.e., the boxed region within the B quadrant of Figure 2). Therefore, our assignment of Met-70 to the boxed region of the B quadrant, indicative of elongated conformation, was based on the large increase in potency observed with peptide 5 in which Gln-71 was substituted with Pro. Pro-71 appeared to fix the preproline residue (Met-70) into a biologically favorable elongated conformation.

Our assignment of Gln-71 to this same region in Ramachandran space came from the NMR data interpretation (see above) and from the analysis of structure-function relationships for peptides 4, 6, and 11. The presence of Pro at position 72 (peptide 4) dramatically decreased potency. This observation, however, is somewhat deceptive because it was influenced much more by the lack of the important contribution made by the side chain of Leu-72 than by a detrimental effect on the preproline residue (Gln-71) being forced into an elongated conformation by the Pro. Second, peptide 6, because of the side-by-side Pro residues, must necessarily have residues 71 and 72 occupying the boxed (elongated) region of quadrant B in Figure 2. In fact, peptide 6 exhibited a reasonable recovery of biological activity, arguing in favor of the backbone of Gln-71 being in an elongated conformation when the more dominating influence of the side chain of Leu-71 is not taken into account. Furthermore, the presence of an Ala at position 72 should disrupt any positive effect the elongation of backbone conformation at position 71 would have on biological activity. In fact, this was observed in peptide 11, where Ala occupies position 72 adjacent to the elongation-inducing Pro at position 71.

Finally, the assignment of residue Leu-72 to the elongated region B in Ramachandran space was based on the enhancement in activity observed with peptide 14, where a D-Pro (already in a favorable stereoisomeric conformation as per D-Ala in peptide 8) occupied position 73. This was also supported by the detrimental effect in activity observed when position 73 is occupied by L-Pro (peptide 3).

Our analysis of the NMR data for human C5a and the positive biological effect of D-Ala substitutions for Gly-73 suggested the possibility of a turn-like motif for the region made up of residues QLGR (residues 71-74). The replacement of Gly-73 with L-Ala (peptide 7) and L-Pro (peptide 3) were both detrimental to biological activity and suggested that the biologically favorable conformation at Gly-73 is not likely to be found in regions B or R in the two, left hand quadrants of Ramachandran space. However, replacement of Gly-73 with D-Ala (peptide 8) and D-Pro (peptide 14) showed

an enhancement in activity and argues strongly in favor of the backbone conformation at position 73 occupying either of the two narrow strips (hashed regions) in the L or H quadrants in the right hand side of Ramachandran space for a biologically favorable conformation. The presence of D-Arg in peptide 22 showed a decrease in spasmogenic activity and argues for the probability of Arg-74 residing in the B or R quarters of Ramachandran space. Thus, backbone conformations of the C-terminal four residues (71, 72, 73, and 74) were assigned to the regions of allowed Ramachandran space corresponding to B, B, L or H, B/R, respectively (see Figure 2). The dihedral combination of B, B, L, B is has been shown to correspond to a type II  $\beta$ -turn and B, B, H, B to a type V  $\beta$ -turn.<sup>39</sup>

In summary, the backbone conformational features that appear responsible for the expression of spasmogenic and platelet aggregatory activities are (i) helix-like conformation for residues (65)66-69, (ii) elongated conformation for residues 70-71, and (iii) a  $\beta$ -turn of either type II or V for residues (71)72-74. These conformational features are shown in Figure 3 for the decapeptide agonist C5a<sub>65-74</sub>Y65,F67 (peptide 2).

**Pharmacological Analysis.** There were significant correlations between  $pD_2$  values for human fetal artery and the assays in guinea pig tissues, as well as with the potencies of analogues in the guinea pig platelet aggregation assay (Figures 4-6). On the basis of these potency correlations among the different assays used in this study, our biological results did not indicate any ability for this series of conformationally constrained analogues to discriminate between the C5a receptors in the differing tissues. These correlations of peptide potencies between spasmogenic and platelet aggregatory assays also provides evidence that a preferred, common conformational motif exists that subserves these biological activities.

The interaction of C5a with its receptor is thought to involve at least three distinct regions of the ligand.<sup>40</sup> However, because our peptides were only a fraction of the size of native C5a (10 vs 74 residues, respectively) and were probably interacting with one specific region of the C5a receptor,<sup>40,41</sup> we could not infer whether the receptors in the various tissues were the same or different. Thus, no evidence for different C5a receptors in these tissues was suggested by our data. Instead, the observed pharmacological correlations for this series of analogues presented in this paper support the hypothesis of a common C5a receptor recognition site in these tissues. It should be noted, however, that some apparent anomalies are evident in our preliminary data. For example, the conformationally constrained peptides 10 and 13 have potencies that differ by about 2 orders of magnitude in the human fetal artery assay, yet are approximately equipotent in the guinea pig platelet aggregation assay. From our results, it is not clear whether this reflects distinctive conformational requirements for receptor interaction in these different tissue types. A more likely explanation may be sampling and/or species variances in the bioassays used in this investigation. Nevertheless, the former possibility cannot be ignored and studies with additional conformationally constrained analogues may lead to a possible subclassification of responses between guinea pig platelets and spasmogenic responses.

Studies with C-terminal agonist peptides in other tissues have resulted in different response patterns depending on the species or assays employed.<sup>25,42,43</sup> Whether these results reflect differences in the C5a receptors expressed in the different cell and tissue systems is presently unclear. It does, however, underscore the appropriateness of using assays with various human cells and tissues if the goal of such studies is the development of a design strategy leading to a clinically useful C5a analogue.

The combined substitution of Pro-71 with D-Ala-73 resulted in the most potent agonist analogues of the present series. The relative potencies of peptides in fetal artery were calculated as the log potency ratios at the EC<sub>50</sub> level compared to C5a. Values were peptide 2, 2.78 ± 0.10 (0.2% of C5a potency); peptide 5, 2.01 ± 0.12 (1%); peptide 10, 1.42 ± 0.13 (4%) (see also Figure 1). Our data also indicate that this panel of constrained decapeptide agonists of C5a interact with C5a receptors from certain cell and tissue types and different species in a homogeneous fashion, suggesting that a common conformational motif may be involved. Whether this is the case for C5a receptors expressed in other cells (e.g. neutrophils) is currently being investigated.

**Summary and Conclusions.** In this paper we have characterized a common, preferred backbone conformation in a series of C-terminal decapeptide agonists of human C5a that correlate with the expression of spasmogenic and platelet aggregatory activities. These structural motifs appear to be a helix-like backbone conformation for residues 65–69, an elongated backbone conformation for residues 70–71, and a  $\beta$ -turn of either type II or V for the region (71)72–74. Indeed, peptides that are conformationally biased toward the expression of these backbone features appear particularly potent in these biological assays. Whether these or other common conformational features will correlate with other patterns of decapeptide agonist-mediated biological responses is currently under investigation.

## Experimental Section

**Structural Interpretation of NMR and Biological Data.** The preliminary estimation of the backbone conformational features of C5a<sub>65–74</sub> and C5a<sub>65–74</sub> analogues was determined by a probabilistic approach<sup>29</sup> utilizing the FISINOE program.<sup>30</sup> FISINOE determines the backbone conformation of a peptide or protein in solution by the Bayesian inferential paradigm by combining NMR data with two-dimensional distribution functions for  $\phi$  and  $\psi$  angles derived from the Protein Data Bank (PDB). In the present case, the sequential *d*-connectivities (SDC) ( $d_{\alpha N}$ ,  $d_{NN}$ , and  $d_{\beta N}$ ) observed in the C-terminal region (C5a<sub>65–74</sub>) for human C5a<sub>26</sub> were used as input data to the FISINOE program. For each amino acid residue within C5a<sub>65–74</sub>, FISINOE calculated the most probable values for  $\phi$  and  $\psi$  angles and their standard deviations that correspond to the given set of SDC.

Further identification/characterization of distinct conformational features in the backbone of the C-terminal decapeptides used in this study was made by a comprehensive analysis of the structure–function relationships with the 23 analogues listed in Table 2. This analysis was made using an approach described by Hruby and Nikiforovich.<sup>39</sup> The SYBYL software package was used for structural visualization of the backbone conformational features determined from the above combined approach. The basic backbone conformational features generated by this analysis are shown for graphical purposes in Figure 3.

**Peptide Synthesis, Purification, and Characterization.** Peptides were synthesized according to standard solid-

phase methodologies on an Applied Biosystems (Foster City, CA) Model 430A peptide synthesizer. Syntheses were performed on a 0.25 mmol scale on [*p*-(hydroxymethyl)phenoxy]methyl]polystyrene (HMP) resins (0.88 mequiv/g substitution). *N*<sup>α</sup>-Amino groups were protected with the base-labile 9-fluorenylmethylloxycarbonyl (Fmoc) group. Side-chain functional groups were protected as follows: Arg (Pmc or 2,2,5,7,8-pentamethylchroman-6-sulfonyl); Asp (O-*tert*-butyl ester); Cys, Gln, & His (Trt or trityl); Lys (Boc or *tert*-butyloxycarbonyl); Ser & Tyr (*tert*-butyl). Synthesis was initiated by the *in situ* coupling of the C-terminal residue (*N*<sup>α</sup>-Fmoc-L-Arg(Pmc)) to the HMP resin in the presence of excess *N,N*-dicyclohexylcarbodiimide (DCC) and 1-hydroxybenzotriazole (HOBT) with 4-(dimethylamino)pyridine (DMAP) as a coupling catalyst. Peptide chain elongation was accomplished by repetitive Fmoc deprotection in 50% piperidine in NMP followed by residue coupling in the presence of 2-(1*H*-benzotriazol-1-yl)-1,1,3,3-tetramethyluronium hexafluorophosphate (HBTU).

Disulfide bridge formation was accomplished by oxidation of the di-Cys(SH) peptide in dilute aqueous solution (0.1 mg/mL, pH 7.5) by K<sub>3</sub>Fe(CN)<sub>6</sub>. The course of disulfide formation was monitored by analytical HPLC. The solution was acidified to pH 3.5 and weakly basic cation exchange beads (Amberlite-HCl IRA-68, Sigma) were added to the solution to form a slurry. The slurry was stirred for 20 min and filtered, and the clear solution was frozen and lyophilized.

Side-chain deprotection and cleavage from the resin were achieved in a single step acidolysis reaction by stirring the peptide-resin in a solution of 84% trifluoroacetic acid (TFA), 6% phenol, 2% ethanediol, 4% thioanisole, and 4% water for 1.5 h at room temperature. Free peptide was precipitated from this solution by adding cold diethyl ether. The mixture was filtered through a sintered glass Buchner funnel (medium porosity) and the peptide/resin washed twice with cold ether to remove the thiol scavengers. The peptide was extracted by swirling the peptide/resin in the funnel with 20–30 mL aliquots of 10% acetic acid followed by filtration. The extraction aliquots were combined, frozen, and lyophilized to yield the powdered form of the crude peptide.

The crude peptide (up to 600 mg) was dissolved in about 100 mL of water and filtered through a 0.45  $\mu$ m nylon filter (Nalgene). Then 10  $\mu$ L of this solution was loaded onto an analytical column (0.5 × 25 cm) packed with C<sub>18</sub>-bonded silica (Isco, Spherisorb 5  $\mu$ m) and eluted with a linear gradient generated from TEAP buffer (0.5% triethylamine (v/v) and 0.5% phosphoric acid (v/v) pH 2.3 (solvent system A) and 60% (v/v) acetonitrile in TEAP pH 2.3 (solvent system B). The gradient (15–45% B over 30 min, flow rate 1 mL/min) was generated by an ABI Model 400 solvent delivery system. The separation was monitored at 214 nm with an ABI Model 783A programmable absorbance detector, and the peaks were recorded and integrated on a Hewlett-Packard 3394A integrator.

Having obtained the analytical chromatogram of the crude peptide, the remainder of the crude solution was loaded onto a radially compressed preparative HPLC column (2.5 × 70 cm) packed with C<sub>18</sub>-bonded silica (Waters DeltaPak 15  $\mu$ m, 300 Å) previously equilibrated with TEAP pH 2.3. The peptide was eluted with a manually-generated gradient of acetonitrile (Waters 590 programmable pump, flow rate 60 mL/min). The preparative gradient was chosen so that the major peptide peak observed in the earlier analytical run of the crude mixture eluted in the mid-region of the chromatographic window. The separation was monitored at two wavelengths—230 nm (Waters 441 Detector) and 214 nm (Gilson 115 UV Detector). Peaks were recorded on a dual pen strip chart recorder (Asea Brown Boveri, SE 120). The major preparative peak was collected and homogeneity verified by analytical HPLC as described above. The preparative column was washed with a column volume of aqueous acetonitrile (70% v/v). Generation of the acetate salt was accomplished by loading the single peptide peak from the TEAP run onto the preparative column previously equilibrated with an aqueous solution of acetic acid (0.5% v/v). The peptide was eluted with a manually generated gradient of acetonitrile in 0.5% aqueous acetic acid at a flow rate of 60 mL/min. The single



peak was collected and purity assessed by analytical HPLC as above. All peptides listed in Table 2 were homogeneous by analytical HPLC analysis of the acetate salt form and were at least 96% pure according to the integrated single peak area. The purified peptide was recovered by lyophilization and further characterized by amino acid compositional analysis and fast atom bombardment mass spectrometry (FAB-MS). These data are consistent with the proposed sequences and are summarized in Table 1.

**Smooth Muscle Contraction Assays.** Tissue strips were suspended in 2 mL organ baths, containing physiological salt solution (Krebs-Ringers solution: 118 mM NaCl, 4.7 mM KCl, 2.5 mM CaCl<sub>2</sub>, 25 mM NaHCO<sub>3</sub>, 1.2 mM KH<sub>2</sub>PO<sub>4</sub>, 1.2 mM MgSO<sub>4</sub>, 10 mM Glucose) maintained at 37 °C, pH 7.4, and continuously aerated with a 95% O<sub>2</sub>/5% CO<sub>2</sub> mixture. Each tissue preparation was equilibrated for 1 h prior to testing with peptides. All drugs were kept on ice during the experiment, and isometric tensions were measured using strain-gauge transducers (Grass FT-03) with a computerized chart recording system (MacLab/8). After the contraction to each peptide reached a plateau, histamine (10 μM) was added to obtain the maximum tissue response. Because tachyphylaxis occurs rapidly to single doses of C5a or peptides, cumulative dose-response curves could not be obtained. Instead, the dose-response profile was compiled from multiple strips from each tissue. After exposing each strip to a single concentration of the peptide followed by supramaximal histamine, the response was expressed as a percentage of the maximal contraction to histamine. Full dose-response curves for C5a (human recombinant C5a; Sigma) or individual peptides were performed in each experiment for each tissue and the EC<sub>50</sub> values (i.e., concentration of peptide producing 50% of the maximal response to each peptide) obtained by probit analysis. pD<sub>2</sub> transforms [-log EC<sub>50</sub> (M)] were calculated for each dose-response curve, and means ± SE obtained for each peptide.

**Human Fetal Artery.** Human umbilical cords were obtained from the Mater Misericordiae Hospital, South Brisbane, Queensland, within minutes of delivery. The mid-section of the umbilical cord was cut from the placenta, placed in physiological salt solution, and stored at 5 °C for up to 24 h. This period of storage did not affect the responsiveness of the tissue to drugs. The fetal arteries were dissected out and cut into longitudinal strips. The intimal surface of the arteries was rubbed with a cotton bud to remove the endothelium. Strips approximately 2 cm × 3 mm were suspended in organ baths under 20 mN of resting tension. Arterial strips were tested repeatedly with peptides following a 60 min drug-free period of rest between assays.<sup>36</sup>

**Guinea Pig Ileum and Lung Parenchyma.** Guinea pigs (250–500 g) of either sex were killed by stunning and exsanguination. The tissues were rapidly removed and placed into chilled (5 °C) physiological salt solutions. Longitudinal strips from the terminal ileum, approximately 2 cm in length, were set up in organ baths with a resting tension of 20 mN. Atropine (0.1 μM) was added to the ileal preparations to reduce spontaneous activity. Lung parenchymal strips were cut from the peripheral edge of the lungs. These strips (1–2 cm × 3–4 mm) were set up with a resting tension of 10 mN. Each ileal and parenchymal strip was tested with peptides one time only.

**Platelet Aggregation Assay.** This assay was performed on platelets obtained from the arterial blood of anesthetized male Hartley guinea pigs according to previously published methods.<sup>23</sup> Briefly, platelet-rich plasma was prepared and diluted to 3 × 10<sup>8</sup> platelets/mL in 0.39% sodium citrate solution. Peptide samples were diluted in a stepwise fashion in 1.5-fold dilutions and placed in 96-well microplates. A 20 mL peptide sample, 80 mL of platelet-rich plasma, and one 3 mm glass bead were placed in each well. The plates were shaken horizontally at 100 rpm for 5 min at 37 °C. Platelet aggregation was evaluated visually in an inverted microscope at 40× magnification. The greatest dilution of peptide producing visible aggregation was scored as the threshold concentration for activity. Natural C5a and C3a were included as internal standards. At least three independent duplicate determinations were conducted for every peptide.

**Abbreviations.** Except where noted, the single letter designation for the amino acid residues are used: A, alanine; C, cysteine; D, aspartic acid; F, phenylalanine; G, glycine; H, histidine; I, isoleucine; K, lysine; L, leucine; M, methionine; N, asparagine; P, proline; Q, glutamine; R, arginine; S, serine; V, valine; Y, tyrosine. Uppercase letters represent the L-amino acid isomer and lowercase the D-isomer.

**Acknowledgment.** We wish to acknowledge the expert technical assistance of Jan Williamson, Dr. Fulvio Perini of the Eppley Institute Molecular Biology Core Laboratory for amino acid analyses, the Midwest Regional Center for Mass Spectrometry, and the theater staff of the Mater Misericordiae Hospital for umbilical tissues.

## References

- (1) Shin, H. S.; Snyderman, E.; Friedman, A.; Mellors, A.; Meyer, M. M. Chemotactic and Anaphylactic Fragments Cleaved from the Fifth Component of Guinea-Pig Complement. *Science* **1968**, *162*, 361–363.
- (2) Hugli, T. E.; Marceau, F.; Lundberg, C. Effects of complement fragments on pulmonary and vascular smooth muscle. *Am. Rev. Respir. Dis.* **1987**, *135*, S9–S13.
- (3) Hugli, T. E.; Muller-Eberhard, J. Anaphylatoxins C3a and C5a. *Adv. Immunol.* **1978**, *26*, 1–53.
- (4) Hugli, T. E. The Structural Basis for Anaphylatoxins and Chemotactic Functions of C3a and C5a. *Crit. Rev. Immunol.* **1981**, *114*, 321–366.
- (5) Hugli, T. E. Structure and Function of C3a Anaphylatoxin. *Curr. Top. Microbiol.* **1990**, *153*, 181–208.
- (6) Goldstein, I. M.; Weissmann, G. Generation of C5a-Derived Lysosomal Enzyme-Releasing Activity (C5a) by Lysates of Leukocyte Lysosomes. *J. Immunol.* **1974**, *113*, 1583–1588.
- (7) Grant, J. A.; Dupree, E.; Goldman, A. S.; Schultz, D. R.; Jackson, A. L. Complement-Mediated Release of Histamine From Human Leukocytes. *J. Immunol.* **1975**, *114*, 1101–1106.
- (8) Schorlemmer, H. U.; Davies, P.; Allison, A. C. Ability of Activated Complement Components to Induce Lysosomal Enzyme Release From Macrophages. *Nature* **1976**, *261*, 48–49.
- (9) Goodman, M. G.; Chenoweth, D. E.; Weigle, W. O. Potentiation of the Primary Humoral Immune Response *In Vitro* by C5a Anaphylatoxin. *J. Immunol.* **1982**, *129*, 70–75.
- (10) Okusawa, S.; Dinarello, C. A.; Yancy, S.; Endres, T. J.; Lawley, T. J.; Frank, M. M.; Burke, J. F.; Garland, J. A. C5a Induction of Human Interleukin 1. Synergistic Effect With Endotoxin or Interferon-γ. *J. Immunol.* **1987**, *139*, 2635–2639.
- (11) Scholz, W.; McClurg, M. R.; Cardenas, G. J.; Smith, M.; Noonan, D. J.; Hugli, T. E.; Morgan, E. L. C5a-Mediated Release of Interleukin-6 by Human Monocytes. *Clin. Immunol. Immunopathol.* **1990**, *57*, 297–307.
- (12) Ember, J. A.; Sanderson, S. D.; Hugli, T. E.; Morgan, E. L. Induction of IL-8 Synthesis From Monocytes by Human C5a Anaphylatoxin. *Am. J. Pathol.* **1994**, *144*, 393–403.
- (13) Chenoweth, D. E.; Goodman, M. G.; Weigle, W. O. Demonstration of a Specific Receptor for Human C5a Anaphylatoxin on Murine Macrophages. *J. Exp. Med.* **1982**, *156*, 67–78.
- (14) Koo, C.; Lefkowitz, R. J.; Snyderman, R. Guanine Nucleotides Modulate the Binding Affinity of the Oligopeptide Chemoattractant Receptor on Human Polymorphonuclear Leukocytes. *J. Clin. Invest.* **1983**, *72*, 748–753.
- (15) Fukuoka, Y.; Neilsen, L. P.; Hugli, T. E. Characterization of the Receptors to the Anaphylatoxins on Isolated Cells. *Dermatologica* **1989**, *179* (suppl. 1), 35–40.
- (16) Gerard, N. P.; Hodges, M. K.; Drazen, J. M.; Weller, P. F.; Gerard, C. Characterization of a Receptor for C5a Anaphylatoxin on Human Eosinophils. *J. Biol. Chem.* **1989**, *264*, 1760–1766.
- (17) Watson, W. C.; Brown, P. S.; Pitcock, J. A.; Townes, A. S. Passive Transfer Studies with Type II Collagen Antibody in B10.D2/Old and New Line and C57B1/6 Normal and Beige (Chediak-Highashi) Strains: Evidence of Important Role for C5 and Multiple Inflammatory Cell Types in the Development of Erosive Arthritis. *Arthritis. Rheumatol.* **1987**, *30*, 460–465.
- (18) Till, G. O.; Johnson, K. J.; Kunkel, R.; Ward, P. A. Intravascular Activation of Complement and Acute Lung Injury. *J. Clin. Invest.* **1982**, *69*, 1126–1135.
- (19) Hammerschmidt, D. E. Activation of the Complement System and of Granulocytes in Lung Injury: The Adult Respiratory Distress Syndrome. *Adv. Inflamm. Res.* **1983**, *5*, 147–172.

- (20) Wingrove, J. A.; DiScipio, R. G.; Chen, Z.; Potempa, J.; Travis, J.; Hugli, T. E. Activation of Complement Components C5 and C5b by a Cysteine Protease (Gingipain-1) From *Porphyromonas (Bacteroides) Gingivalis*. *J. Biol. Chem.* **1992**, *267*, 18902–18907.
- (21) Siefert, P. S.; Kazatchkine, M. D. Generation of Complement Anaphylatoxin and C5b-9 by Crystalline Cholesterol Oxidation Derivatives Depends on Hydroxyl Group Number and Position. *Mol. Immunol.* **1987**, *24*, 1303–1308.
- (22) Schafer, H.; Mathey, D.; Hugo, F.; Bhakdi, S. Deposition of the Terminal C5b-9 Complement Complex in Infarcted Areas of Human Myocardium. *J. Immunol.* **1986**, *137*, 1945–1949.
- (23) Ember, J. A.; Sanderson, S. D.; Taylor, S. M.; Kawahara, M.; Hugli, T. E. Biologic Activity of Synthetic Analogues of C5a Anaphylatoxin. *J. Immunol.* **1992**, *148*, 3165–3173.
- (24) Morgan, E. L.; Sanderson, S. D.; Scholz, W.; Noonan, D. J.; Weigle, W. O.; Hugli, T. E. Identification and Characterization of the Effector Region Within Human C5a Responsible for Stimulation of IL-6 Synthesis. *J. Immunol.* **1992**, *148*, 3937–3942.
- (25) Drapeau, G.; Brochu, S.; Godin, D.; Levesque, L.; Rioux, F.; Marceau, F. Synthetic C5a Receptor Agonists: Pharmacology, Metabolism and *In Vivo* Cardiovascular and Hematological Effects. *Biochem. Pharmacol.* **1993**, *45*, 1289–1299.
- (26) Zuiderweg, E. R. P.; Nettesheim, D. G.; Mollison, K. W.; Carter, G. W. Tertiary Structure of Human Complement Component C5a in Solution from Nuclear Magnetic Resonance Data. *Biochemistry* **1989**, *28*, 172–185.
- (27) Sanderson, S. D.; Sherman, S. A.; Gmeiner, W.; Ember, J. A.; Taylor, S. M. Conformational Features of Biological Activity in C-Terminal Agonist Peptides of Human C5a. Abstract presented at the 13th American Peptide Symposium, June 20–25, 1993, poster 367.
- (28) Taylor, S. M.; Finch, A. M.; Sherman, S. A.; Sanderson, S. D. Restriction of Flexibility in the Carboxyterminal Region of C5a Analogues Affects Potency. *Clin. Exp. Pharm. Physiol. Suppl. 1* **1993**, A72.
- (29) Sherman, S. A.; Johnson, M. E. Derivation of Locally Accurate Spatial Protein Structure from NMR Data. *Prog. Biophys. Mol. Biol.* **1993**, *59*, 285–339.
- (30) Sherman, S. A.; Johnson, M. E. Estimation of Accuracy in Determining Protein Backbone Conformations from NOE Data and Empirical  $\phi, \psi$  Probability Distributions. *J. Magn. Reson.* **1992**, *96*, 457–472.
- (31) Wurtrich, K. *NMR of Proteins and Nucleic Acids*; John Wiley and Sons: New York, 1986; pp 162–175.
- (32) Kawai, M.; Quincy, D. A.; Lane, B.; Mollison, K. W.; Or, Y.-S.; Luly, J. R.; Carter, G. W. Structure-Function Studies in a Series of Carboxyl-Terminal Octapeptide Analogues of Anaphylatoxin C5a. *J. Med. Chem.* **1992**, *35*, 220–223.
- (33) Mollison, K. W.; Fey, T. A.; Krause, R. A.; Miller, L.; Edalji, R. P.; Conway, R. G.; Mandecki, W.; Shallcross, M. A.; Kawai, M.; Or, Y.-S.; Lane, B.; Carter, G. W. C5a Structural Requirements for Neutrophil Receptor Interaction. *Agents Actions, Suppl.* **1991**, *35*, 17–21.
- (34) Or, Y.-S.; Clark, R. F.; Lane, B.; Mollison, K. W.; Carter, G. W.; Luly, J. R. Improvements in the Minimum Binding Sequence of C5a: Examination of His-67. *J. Med. Chem.* **1992**, *35*, 402–406.
- (35) Bodammer, G.; Vogt, W. Contraction of Guinea-Pig Ileum Induced by Anaphylatoxin Independence of Histamine Release. *Int. Arch. Allergy* **1970**, *39*, 648–657.
- (36) Taylor, S. M.; Finch, A. M.; Heron, A. E.; Brown, L. C.; Florin, T. H. J. Reversibility of Tachyphylaxis to C5a in Guinea-Pig Tissues, the Perfused Human Placental Lobule, and the Umbilical Artery. *Inflammation*. In press.
- (37) Marceau, F.; Blois, D. D.; Laplante, C.; Pettitclerc, E.; Pelletier, G.; Grose, J. H.; Hugli, T. E. Contractile Effect of the Chemotactic Factors f-Met-Leu-Phe and C5a on the Human Isolated Umbilical Artery. *Circ. Res.* **1990**, *67*, 1059–1070.
- (38) Stimler, N. P.; Brocklehurst, W. E.; Bloor, C. M.; Hugli, T. E. Anaphylatoxin-Mediated Contraction of Guinea-Pig Lung Strips: A Non-Histamine Tissue Response. *J. Immunol.* **1981**, *126*, 2258–2261.
- (39) Hruby, V. J.; Nikiforovich, G. V. The Ramachandran Plot and Beyond: Conformational and Topochemical Considerations in the Design of Peptides and Proteins. In *Molecular Conformation and Biological Interactions*; Balaram, P., Ramasehan, S., Eds.; Indian Academy of Sciences: Bangalore, 1991; pp 429–445.
- (40) Mollison, K. W.; Mandecki, W.; Zuiderweg, E. R. P.; Fayer, L.; Fey, T. A.; Krause, R. A.; Conway, R. G.; Miller, L.; Edalji, R. P.; Shallcross, M. A.; Lane, B.; Fox, J. L.; Greer, J.; Carter, G. W. Identification of Receptor Binding Residues in the Inflammatory Complement Protein C5a by Site-Directed Mutagenesis. *Proc. Natl. Acad. Sci. U.S.A.* **1989**, *86*, 292–296.
- (41) Siciliano, S. J.; Rollins, T. E.; DeMartino, J.; Konteatis, Z.; Malkowitz, L.; VanRiper, G.; Bondy, S.; Rosen, H.; Springer, M. S. Two-Site Binding of C5a by its Receptor: An Alternative Binding Paradigm for G-Protein-Coupled Receptors. *Proc. Natl. Acad. Sci. U.S.A.* **1994**, *91*, 1214–1218.
- (42) Mollison, K. W.; Krause, R. A.; Fey, T. A.; Miller, L.; Wiedeman, P. E.; Kawai, M.; Lane, B. Hexapeptide Analogues of C5a Anaphylatoxin Reveal Heterogeneous Neutrophil Agonism/Antagonism. *FASEB J.* **1992**, *6*, A2058.
- (43) Fey, T. A.; Mollison, K. W.; Krause, R. A.; Miller, L.; Kawai, M.; Lane, B.; Luly, J. R.; Carter, G. W. Heterogeneity in Chemokinetic and Enzyme Release Efficacy of C5a Analogues Across Multiple Species. *FASEB J.* **1992**, *6*, A2058.